

## Multi-parameter optimization of layered hBN/PMMA nanocomposite under mechanical loading

T. Petrova<sup>1\*</sup>, E. Kirilova<sup>1</sup>, R. Vladova<sup>1</sup>, A. Apostolov<sup>1</sup>, B. Boyadjiev<sup>1</sup>, A. Moravski<sup>2</sup>

<sup>1</sup>

*Institute of Chemical Engineering, Bulgarian Academy of Sciences, Acad. G. Bonchev Str., Bl. 103, 1113 Sofia, Bulgaria*

<sup>2</sup>*Faculty of Mathematics and Informatics, Sofia University "St. Kliment Ohridski", 5 James Bourchier Blvd., 1164 Sofia, Bulgaria*

Received June 3, 2024; Accepted: August 17, 2024

In the present study, a methodology is proposed to find the optimal safe values for the geometry and the magnitude of the axially applied mechanical load for hBN/PMMA nanocomposite, so as to avoid the possibility of its delamination/fracture, by using Genetic Algorithms. First, the analytical solutions for the interface shear stress in the middle layer of the considered nanostructure are obtained, based on the application of the 2D method of the stress function and the minimization of the strain energy. Second, the theoretical criterion for no delamination in the interface layer, based on the model ISS is formulated, including the structure geometry and loading as parameters. The multi-parameter optimization problem involving this criterion is then defined and solved by the GA. By varying all parameters simultaneously, their safety intervals (without delamination) in the considered nanocomposite structure are obtained. The magnitude of the applied load was found to mainly affect the magnitude of the ISS. Layer thicknesses mostly affect the type of ISS solution, especially the substrate thickness. The effect of layer length on ISS is weaker than that of layer thickness at fixed load. The obtained results can be used for fast delamination prediction and appropriate design in such nanostructured devices to ensure their safe operation.

**Keywords:** Multi-parameter optimization, hBN/Interface/PMMA nanocomposite, interface shear stress, delamination

### INTRODUCTION

Boron nitride nanosheet (BNNS)-polymer composites are one of the important classes of materials with a wide range of applications: automotive, aerospace, energy storage [1], medicine, electronic engineering, etc. Properties of the hBN/polymer nanocomposites mainly depend up on filler size and dispersion, mixing conditions and type of interaction between polymer matrix and the nano filler [2]. Boron nitride (BN) nanomaterials have superior fracture strength (165 GPa), high Young's modulus (0.8 TPa), high thermal stability (up to 800 °C in the air), excellent thermal expansion coefficient ( $-2.72 \times 10^{-6} \text{ K}^{-1}$ ), and outstanding thermal conductivity (300–2000  $\text{W m}^{-1} \text{ K}^{-1}$ ) [3]. Among the abovementioned BNNS properties, in this review work [3], the fundamental parameters that control the molecular interactions of BNNSs with polymer matrices have been considered in detail. The authors take into account two groups of factors influencing the hBN/polymer nanocomposites properties – non-interfacial and interfacial factors. The latter ones show a strong effect on the stress-transfer efficiency of this kind of

nanocomposites and include: covalent and non-covalent interactions at the interfacial surface area, and at the BNNS-polymer interface. A transitional zone is created, termed as „interphase“, which is the origin of property changes in polymer nanocomposites. Interphases have a vital role in transferring mechanical stress, thermal heat, and electrical load from one phase into another.

At the moment, scientists still do not have a direct method to experimentally measure and determine the properties and geometrical characteristics (thickness, length, etc.) of such an interphase zone not only for (BNNS)-polymer, but also for the recently widespread nanocomposites of other 2D materials (graphene, MoS<sub>2</sub>, WS<sub>2</sub>, Mxenes, etc.) and different substrates [4-6]. There are several theoretical developments that attempt to fill this lack of information about the interphase zone. In the dissertation of Kochetov [7], the Lewis-Nielsen model was used with a third phase (interface) added to the other two – spherical/platelet nanoparticles of BN and an epoxy matrix, to explain the Kapitza's resistance of an interphase boundary phenomenon and its influence on thermal conductivity. Kochetov has proved that such a phase must exist, since accounting for it yields realistic thermal conductivity values compared to experimental data, unlike the

\* To whom all correspondence should be sent:

E-mail: [t.petrova@iche.bas.bg](mailto:t.petrova@iche.bas.bg)

case of only two phases in the model. Kochetov's model yielded the following values for the width of the interface zone:  $1.6 \div 2.5$  nm. This author also mentioned that for a polymer/nanoclay the width of this zone is  $5 \div 15$  nm and for PVA/Si nanocomposites it is  $5 \div 10$  nm.

Later, the scientists' interest to hBN/polymer or other nanocomposites, as well as to the interface zone between them, increased: hBN/epoxy [8], hBN/Si [9], hBN/PDMS [10], BNNT/PMMA [11], hBN/PMMA [12], hBN/PVA [13], and hBN/sapphire [14]. But only in [8], [9] and [11], the interface area has also been considered and studied. In [11], the load transfer characteristics of boron nitride nanotube (BNNT)/PMMA interfaces by using a micromechanic shear-lag model that takes into account the elastoplastic properties of polymer matrices, have been investigated. Closed-form analytical solutions of the interfacial shear stress distribution profile are derived. The failure of the nanotube-polymer interface and the pull-out force are analyzed using this strain-hardening model based on recently reported nanomechanical single-nanotube pull-out experiments. The BNNT/PMMA interface is found to possess a maximum interface shear strength (IFSS) of  $71 \pm 2$  MPa that is predicted using the strain-hardening model, as compared to  $236 \pm 11$  MPa that is predicted using the elastic model. The thickness of interface matrix layer is fixed in this model as 8.05 nm. In the paper of Yi *et al.* [9] on hBN/Si, the maximum IFSS is 1.25 GPa, unlike much lower values of IFSS in the literature for BNNT/PMMA – 219 MPa and for BNNT/epoxy – 323 MPa. In [9] the thickness of interface layer is 8.1 nm, which is very close to the value in [11]. In contrast to the latter one, in [9] the authors have obtained the interphase thickness of hBN/epoxy to be 0.6 Å (0.06 nm) and IFSS 9.5 MPa. When the surface of hBN is functionalized with additional groups (4 and 8), the IFSS increased from 13.9 to 17.7 MPa. Their results indicate that the interface region of BNNS/EP is composed of three regions, namely, compact region, buffer region, and normal region. As a conclusion, one might say that there are no papers, which discussed the influence of geometry and material properties of interface layer (zone) on the value of ISS in the available literature. Also, there are no studies, in which an optimization of the hBN/polymer nanocomposite geometry is

done, in order to obtain the best stress transfer without failure /delamination. Our contribution to the researches on the above topic has been reported recently [15]. The most important parameters, which influenced the value of ISS, have been theoretically determined by parametric analysis: the magnitude of external load, the thicknesses of the layers and the length of nanocomposite structure hBN/Interface/PMMA. The analytical model results for strain in hBN and ISS are validated successfully in the elastic zone of external loads with experimental data of [12]. After this short literature analysis, it is well established that the reinforcement of polymers by hBN nanofillers is controlled by stress transfer from the matrix to the reinforcement. Also, it is obvious that the existence and consideration of the interface is essential to the stress transfer between the two other phases. One of the most important requirements from the industry applications of the nanostructures is to assure their safe design and loading.

The aim of this work is to find the optimal values of geometry (length and thicknesses of all three layers), as well as the maximal value of external load at the example of hBN/Interface/PMMA nanocomposite under mechanical loading, without delamination in it. Combining 2D stress-function model predictions for interface shear stress [16] and Genetic Algorithm optimization procedure [17], different optimal sets of geometry configurations of the layers (length and thicknesses of all three layers) and maximal load in the considered nanocomposite structure, have been obtained. The objective function in GA multi-parameter problem is the criterion for “no delamination” in the structure, requiring ISS to be less or equal to ultimate shear stress at the interface layer. The novelty of the present work is to find all optimal values of geometry and load parameters simultaneously, which becomes possible by the metaheuristic GA approach used.

#### MATHEMATICAL MODEL

The formulation and derivation of analytical solutions for stresses (and strains) in a 3-layer nanocomposite structure (Fig. 1) by 2D stress-function method were already published in detail in [16]. Here only the most important formulas will be given.

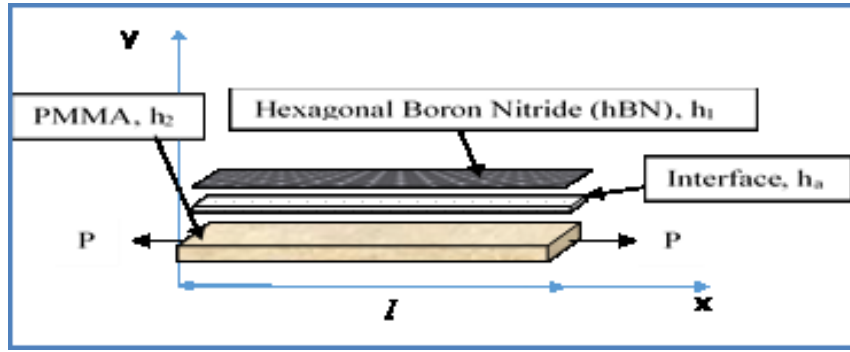


Fig. 1. Representative volume element (RVE) of a 3-layer hBN/Interface/PMMA nanocomposite structure.

According to the model assumptions, all axial stresses in the layers are functions of axial coordinate  $x$  only. Also, the axial stress in the interface layer is set negligible in respect to the same ones in the other two layers. Applying the 2D stress-function method, one can obtain a 4th order differential equation (ODE) with constant coefficients, with respect to the unknown axial stress function  $\sigma_1$  in the first layer (nanolayer). Two types of analytical model solutions for the axial stress  $\sigma_1$  in the nanolayer are derived, with coefficients depending from the geometry of the three-layer nanocomposite, its material properties and external load:

$$\sigma_1(x) = C_1 \exp(\lambda_1 \cdot x) + C_2 \exp(\lambda_2 \cdot x) + C_3 \exp(\lambda_3 \cdot x) + C_4 \exp(\lambda_4 \cdot x) - A \quad (1)$$

$$\sigma_1(x) = \exp(-ax)[M_1 \cos(\beta x) + M_2 \sin(\beta x)] + \exp(ax)[M_3 \cos(\beta x) + M_4 \sin(\beta x)] - A \quad (2)$$

In eqs. (1) and (2) the constant  $A$  is the solution for non-homogeneous ODE and depends on the external static load ( $\sigma_0 = P/h_2$ ), and  $C_i$  and  $M_i$  are the integration constants in the model solutions, determined from the respective boundary conditions [16]. All other stresses in the layers, including the interface shear stress (ISS), are expressed by eqs. (1) or (2) and its derivatives. Eq. (2) is the solution for a case of 4 complex roots  $\pm(\alpha \pm i\beta)$ , while eq. (1) corresponds to the case of 4 real roots  $\lambda_i$ . It is worth noting [16] that the type of roots depends on the chosen geometry of the nanocomposite structure (layers' thickness and length).

The model criterion for no interface delamination in the nanostructure was defined, where USS is the ultimate shear stress of interface (adhesive) layer:

$$\sigma_{xy}^{(a)}(x) = h_1 \sigma_1' \leq \sigma_{USS}^{(a)} \quad (3)$$

Graphically, if exists, the delamination starts at both ends of the nanostructure and represents the intersection of the ISS model curve with the straight horizontal line corresponding to the USS.

## MULTI-PARAMETER OPTIMIZATION

## PROBLEM

The genetic algorithm (GA) known as BASIC GA [17] was employed to tackle the formulated below multi-parameter optimization problems. Here, only a short overview on the working steps for GA application is presented.

In the initial iteration called "a generation" in terms of the genetic algorithms, BASIC GA initializes a "population" (set) comprising randomly generated solutions (vectors of values for the control variables), called "chromosomes" or "individuals". The GA operates with a constant, predefined population size that remains unchanged within the searching process. The solutions are represented by their genotype and the search is performed in the continuous space. Through the application of so called "morphogenesis" functions, solutions are transformed (coded) from their genotype to their "phenotype". The latter is needed to compute the values of both the objective functions (OF) of the chromosomes and their "fitness" functions. The fitness function represents a normalized objective function. Following this, genetic operators are applied to the individuals from the population. These operators are "selection for reproduction (crossover)", "reproduction (crossover)", "mutation," and finally, "selection to replacement" as in which the old individuals (from the previous generation) are replaced with the newly created "offspring" (for details see [17]).

At first, a selection for reproduction is carried out. Subsequently, the mutation operator is applied. In the final stage, selection for replacement is carried out to generate a new population for the next generation. A morphogenesis function is applied to the offspring to derive the solutions in their phenotype. Then, the objective functions of all solutions in the pool are computed. The best-value solution for the OF is selected to pass into the new generation. The replacement selection applied is unbiased, meaning the next generation of solutions is augmented to the specified number with solutions randomly selected from the pool. At the conclusion

of this final stage, the number of generations increases. As a criterion for stopping the search, BASIC GA uses reaching a predefined number of generations.

The BASIC GA encompasses various types of genetic selection operators for reproduction, crossover, and mutation, offering users the flexibility to choose among them to address a specific optimization problem. Moreover, the BASIC GA is designed to handle constrained optimization problems by employing penalty functions.

For the considered nanocomposite hBN/Interface/PMMA structure, the goal is to find simultaneously the optimal values of the control variables (length, thicknesses of layers  $h_1$ ,  $h_a$ ,  $h_2$  and external load  $\sigma_0$ ), at which the OF – eq. (3) has the minimum value, less or equal to USS. The control variables are in preliminary defined boundaries (upper and lower) which are physically and technologically correct. The so formulated multi-parameter optimization problem (MPOP) is solved by GA approach for various combinations of selections methods, type of recombination and mutation used. Also, the number of populations, samples and generations are varied too during the optimization procedure. The results can be seen in

Table 1. As a stop criterion the number of generations (iterations) is used.

Meanwhile, an alternative optimization procedure was developed especially for the case of real roots solution – eq. (1) for ISS in the OF. During the optimization, the GA proved to be more suitable for finding the optimal values of the control variables in the case of OF (or ISS) calculated for complex roots - eq. (2). For real roots case for ISS (eq. (1)), the strong requirement for equality in minimization of OF (eq. (3)) makes finding of optimal values of variables in some cases yet impossible or needs too many efforts and computing time. That's why the alternative optimization procedure in Wolfram Mathematica 13.0.1 has been developed (Fig. 2(a)) which offers a solution of the abovementioned problem. Here, different sets of geometry are included in the optimization cycle for the external load, checking if OF is fulfilled or not at the current values of parameters; it's repeated as many times as needed by the user up to reaching close to the optimal solutions. The important model assumption that the axial stress in the interface layer is negligible in respect to the same ones in the other two layers, is additionally checked (Fig. 2(b)). The obtained results are presented in Table 2.

**Table 1.** Optimal values of control variables from GA for hBN/Interface/PMMA (complex roots)

Solution No.	Optimal load $\sigma_0$ , (Pa)	Optimal length $l$ , (m)	Optimal $h_1$ , (m)	Optimal $h_a$ , (m)	Optimal $h_2$ , (m)	GA population, samples, generations numbers	Methods and schemes used in GA*
1	5.52E+09	2.42E-05	2.83E-09	3.31E-08	6.61E-04	300/100/100	TS, AC, NM
2	4.92E+09	2.73E-05	1.95E-09	9.15E-09	7.17E-04	300/100/500	TS, AC, NM
3	4.55E+09	2.13E-05	4.10E-09	1.51E-09	5.44E-04	500/100/500	TS, AC, NM
4	1.73E+09	2.55E-05	1.69E-09	3.17E-08	4.71E-04	500/200/500	RS, AC, NM
5	1.73E+09	2.55E-05	1.69E-09	3.17E-08	4.71E-04	500/200/500	RS, AC, UM
6	3.20E+08	8.31E-05	2.80E-09	4.40E-09	8.62E-04	500/200/500	RWS, TPC, NM
7	3.30E+08	8.31E-05	1.46E-09	3.51E-09	8.62E-04	500/200/500	RWS, UC, BMD
8	3.25E+08	8.31E-05	1.46E-09	4.16E-09	8.57E-04	500/200/500	RWS, BC, PBMD
9	5.57E+09	2.25E-05	5.00E-09	1.00E-09	6.14E-04	500/200/500	RWS, OPC, NM
10	3.29E+08	8.31E-05	1.46E-09	4.27E-09	8.61E-04	500/200/500	RWS, UC, PBMD
11	2.07E+09	3.18E-05	5.57E-10	9.66E-08	7.87E-04	500/200/500	RWS, UC, PBMD
12	1.60E+09	2.04E-05	3.03E-09	3.18E-08	4.22E-04	500/200/500	RWS, UC, PBMD
13	1.71E+09	2.13E-05	1.54E-09	3.21E-08	4.32E-04	500/200/500	TS, AC, NM

\* Tournament selection, Arithmetical crossover, Nonuniform mutation (TS, AC, NM);

Rank selection, Arithmetical crossover, Nonuniform mutation (RS, AC, NM);

Rank selection, Arithmetical crossover, Uniform mutation (RS, AC, UM);

Roulette wheel selection, Two-points crossover, Nonuniform mutation (RWS, TPC, NM);

Roulette wheel selection, Uniform crossover, Parameter based mutation Deb (RWS, UC, PBMD);

Roulette wheel selection, Blend crossover, Parameter based mutation Deb (RWS, BC, PBMD);

Roulette wheel selection, One-point crossover, Nonuniform (RWS, OPC, NM);

Roulette wheel selection, Uniform crossover, Parameter based mutation Deb (RWS, UC, PBMD).

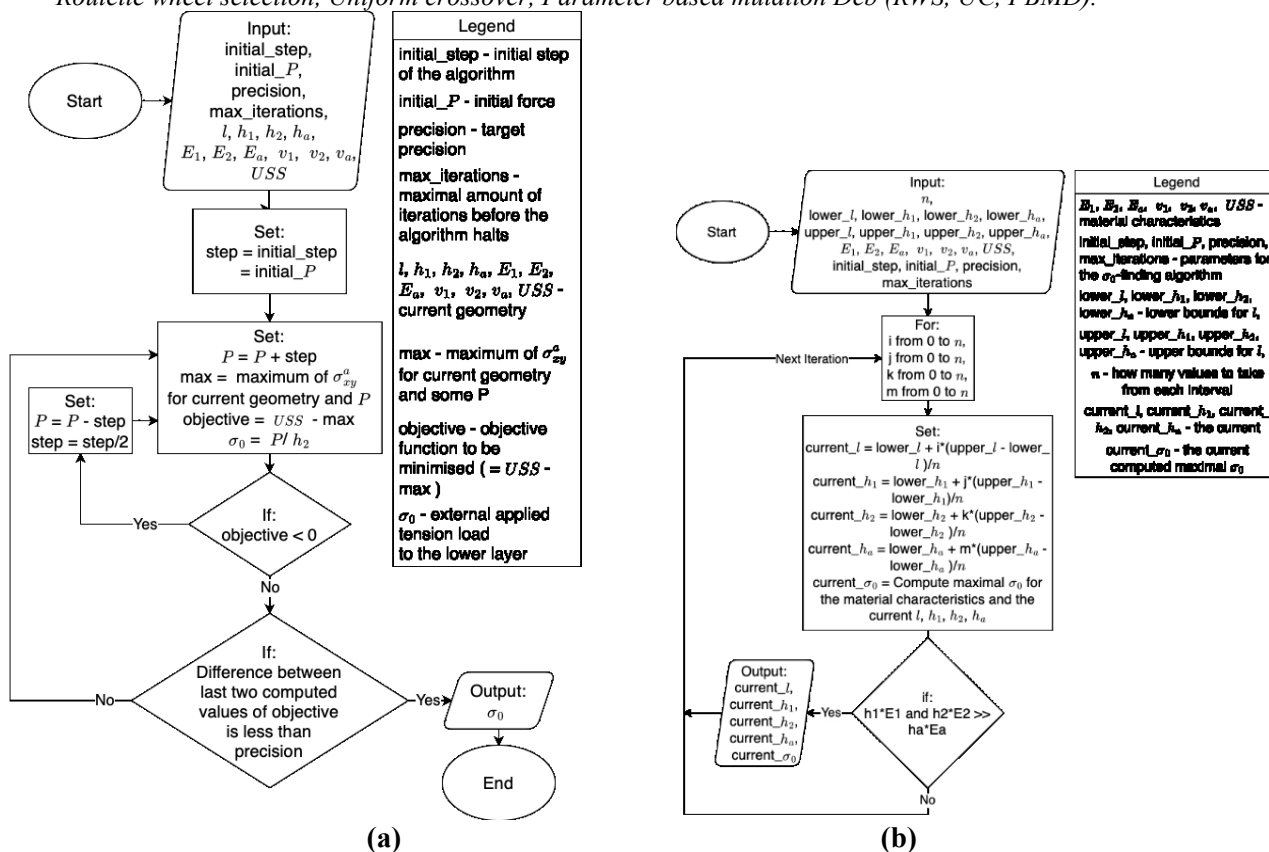


Fig. 2. Schemes of optimization algorithm - (a), and checking of model assumptions for the axial stress in the interface layer - (b).

Table 2. Optimal values of parameters from Mathematica optimization procedure for hBN/Interface/PMMA (real roots)

Solution** No.	M2	M6	M10	M14
Optimal load $\sigma_0$ , MPa	209	113	209	113
Optimal $l$ , m	1e-05	1e-05	2e-05	2e-05
Optimal $h_1$ , m	3.5e-10	1e-09	3.5e-10	1e-09
Optimal $h_a$ , m	1e-08	1e-08	1e-08	1e-08
Optimal $h_2$ , m	1e-06	1e-06	1e-06	1e-06

\*\* to differentiate the solutions in graphic results, these from Mathematica are noted with M

## RESULTS AND DISCUSSION

The material properties: Young modulus  $E$ , (Pa) and Poisson ratio  $\nu$ , (-) of the considered nanocomposite structure (Fig. 1) hBN/Interface/PMMA are taken from [12] as:  $E(\text{hBN})=600$  GPa,  $E(\text{Interface}) = 3.5$  (GPa),  $E(\text{PMMA}) = 3.5$  GPa,  $\nu(\text{hBN}) = 0.21$ ,  $\nu(\text{Interface}) = 0.25$ ,  $\nu(\text{PMMA}) = 0.35$ . Each of the control variables

is fixed in preliminary boundaries (intervals) for optimization procedures.

For the model ISS and GA optimization calculations authors' programs in Mathcad Prime v.6.0 (for complex roots case) and in Wolfram Mathematica 13.0.1 (for real roots case), have been created. The figures are prepared in Sigma Plot, v.13.0.

In Fig. 3, the optimal values of the parameters (load, length, thicknesses of the three layers) obtained in the two optimizations carried out with criterion equation (3), are plotted by two distinct colors symbols. It can be seen that along the ordinate each parameter changes within certain limits (intervals) for each of the two types of solutions (1) and (2) for ISS included in criterion (3).

The limits of the changes of the optimal thicknesses of PMMA  $h_2$  and of the interface layer  $h_a$ , for the cases of real and complex roots, are particularly well differentiated (see the ellipses in blue and red in Fig. 3). The intervals of variation of  $h_1$  (triangles down) and  $l$  (circles) are almost similar for both possible solutions (1) and (2). On the abscissa, each different set of 4 geometry data corresponds to a unique mechanical load such that for each group of five parameters criterion (3) is met or the model-predicted ISS at these load and geometry values is equal to or below the critical USS value.

In order to verify the obtained results, the following Figures 4 and 5 present a part of the

distributions of the ISS along the length of the nanocomposite, obtained at the optimal values of the parameters. As can be seen, for each type of solution, model ISS, calculated at the optimal values of the studied parameters actually meet the criterion of not having delamination in the nanocomposite structure. For the case of ISS, calculated by Mathematica for real roots eq. (1) (Fig. 5), it is worth noting that these optimal values assure that ISS is far from USS, e.g., this geometry and load assure more safety design in comparison with the case ISS for complex roots (Fig. 4).

Given the fact that there are no known experimental ISS data to compare with in the available literature, when such data become available in the future, it will be possible to further validate the results obtained here.

The only data which can be compared, is the thickness of interface layer – our common interval of obtained optimal values for  $h_a$  (m) for both cases of model ISS (real and complex) is  $(1e-09 \div 9.6e-08)$ .

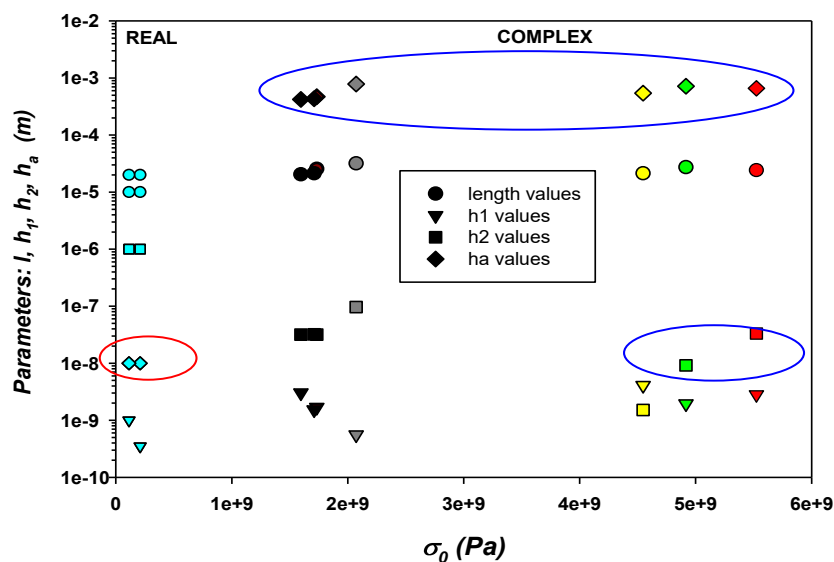


Fig. 3. Optimal solutions for 5 parameters from GA and Mathematica: complex (incrementing) and real roots (Cian)

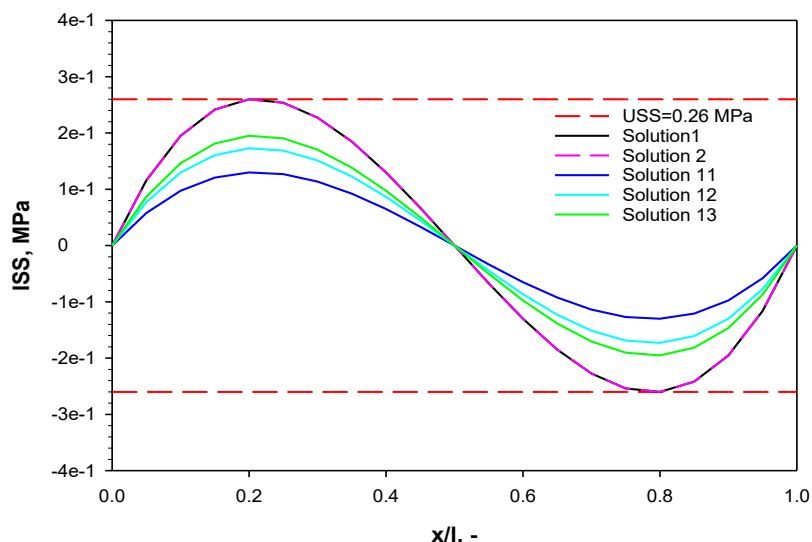


Fig. 4. Model interface shear stress distribution calculated by the optimal values of parameters (complex roots) for considered nanocomposite.

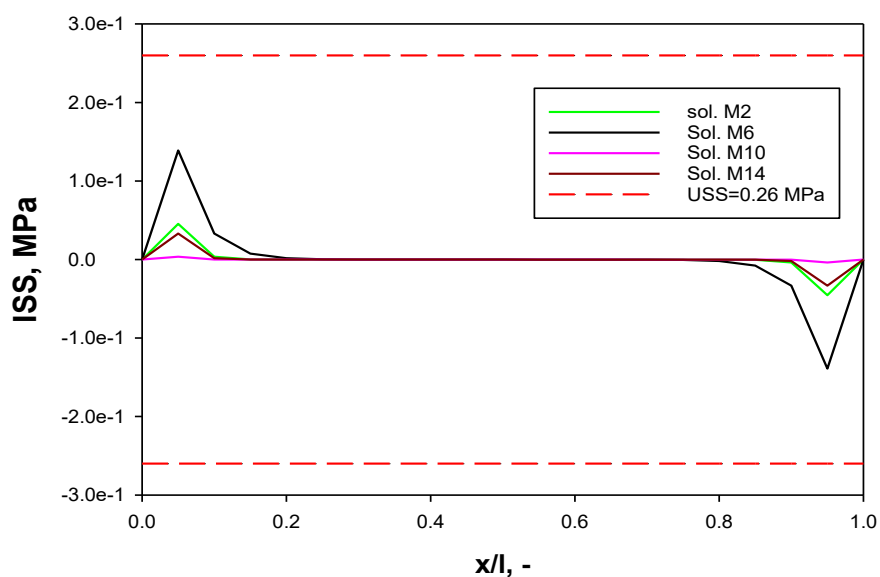


Fig. 5. Model interface shear stress distribution calculated at the optimal values of parameters (real roots) by Mathematica

It is worth noting that the values obtained by Gou *et al.* 2019 [11] (8.05 nm) and by Yi *et al.*, 2019 [9] (8.01 nm), as well as these of Kochetov [7] (1.6÷2.5 nm), are all within the range of the obtained here optimal results for interface thickness  $h_a$ , no matter that different substrates are used in combination with hBN.

### CONCLUSIONS

Here, the 2D stress-function model, combined with GA approach, was successfully applied for the first time to find, optimize and predict the safety load and geometry design of hBN/Interface/PMMA nanocomposite subjected to a static extension load.

The analytical model criterion without delamination in the considered nanocomposite, was

used as an objective function in two formulated multi-parameter optimization procedures for 5 parameters – 4 geometrical and 1 for mechanical loading. The five-parameter optimization problem for nanostructure safety work (without delamination) was formulated and solved with GA approach and Mathematica for hBN/Interface/PMMA.

The possible optimal solutions from GA and Mathematica represent sets of different combinations of all 5 parameters, which vary within predefined boundaries, according to physical and technical prescriptions. The results show that at the obtained optimal values of parameters the model ISSs confirmed and graphically fulfilled the model criterion of no delamination in the



hBN/Interface/PMMA nanocomposite. The obtained here results for the interval of optimal thickness for the interface layer  $h_a$  are in very good coincidence with available literature data for interface thickness in hBN/substrate nanocomposites.

The here proposed methodology for determining and predicting the optimal geometry design and load can be applied to any material combinations for three-layer nanocomposite structures, which satisfy the model assumptions [16].

**Acknowledgement:** This study is performed by the financial support under the contract No. KII-06-H57/3/15.11.2021 with Bulgarian National Science Fund for the project „Optimal safe loads and geometry for layered nanocomposites under thermo-mechanical loading “.

#### Nomenclature

$A$	constant, solution of non-homogeneous ODE of 4 <sup>th</sup> order in [16];
$C_i, M_i$	integration constants in the model solutions, determined from the respective boundary conditions [16];
$E$	Young modulus of a layer material, Pa;
$h_1, h_a, h_2$	thicknesses of the 1 <sup>st</sup> , interface and 2 <sup>nd</sup> layers in the nanocomposite (Fig. 1), $m$ ;
ISS	model interface shear stress, eq. (3), Pa;
$l$	length of the nanocomposite (Fig. 1), $m$ ;
$P$	applied tension force to the substrate (Fig. 1), $N.m$ ;
$x, y$	coordinate system (Fig.1), $m$ ;
USS	ultimate shear stress of interface layer in nanocomposite, Pa.

#### Greek symbols

$\alpha \pm i\beta$	complex roots of the characteristic equation, corresponding to ODE of 4 <sup>th</sup> order in [16];
$\lambda_i$	real roots of the characteristic equation, corresponding to ODE of 4 <sup>th</sup> order in [16];
$\nu$	Poisson number (ratio), -;
$\sigma_0 = P/h_2$	external loading stress applied to substrate (Fig. 1), Pa;
$\sigma_1, \sigma_{x,y}^a$	model [16] axial and shear stress in eqs. (1), (2) and (3), Pa.

#### Abbreviations

BN/BNNS Boron nitride/Boron nitride nanosheet;

BNNT	Boron nitride nanotubes;
GA	genetic algorithm;
hBN	hexagonal boron nitride;
ISS/USS	Interface/Ultimate shear stress;
IFSS	Interface shear strength;
$M2, M6,$	optimal solutions from the
$M10, M14$	optimization procedure in Mathematica, (Table 2);
ODE	ordinary differential equation;
OF	objective function [17];
PDMS	Polydimethylsiloxane, silicone polymer;
PMMA	Poly(methyl methacrylate), plexiglas or acrylic;
PVA	Polyvinyl alcohol, synthetic polymer.

#### REFERENCES

1. W. Liu, B. Ullah, Ch.-Ch. Kuo, X. Cai, *Advances in Polymer Technology*, **2019**, Article ID 4294306, (2019). <https://doi.org/10.1155/2019/4294306>
2. J. Joy, E. George, P. Haritha, S. Thomas, S. Anas, *J. Polym. Sci.*, **58**, 3115 (2020). <https://doi.org/10.1002/pol.20200507>
3. M. G. Rasul, A. Kiziltas, B. Arfaei, R. Shahbazian-Yassar, *2D Materials and Applications*, **5**, article No. 56 (2021). <https://doi.org/10.1038/s41699-021-00231-2>
4. K. Bera, D. Chugh, A. Patra, H. H. Tan, C. Jagadish, A. Roy, *ArXiv preprint arXiv:1907.05591*, (2019). <https://doi.org/10.48550/arXiv.1907.05591>
5. S. S. Akhtar, *Polymers*, **13**, 807 (2021). <https://doi.org/10.3390/polym13050807>
6. M. E. P. Tweedie, Y. Sheng, S. G. Sarwat, W. Xu, H. Bhaskaran, J. H. Warner, *ACS Appl. Mater. Interfaces*, **10**(45), 39177 (2018). <https://doi.org/10.1021/acsami.8b12707>
7. R. Kochetov, PhD thesis, Technische Universiteit Delft, The Netherlands, 2012. [https://www.researchgate.net/publication/241862538\\_Thermal\\_and\\_Electrical\\_Properties\\_of\\_Nanocomposites\\_Including\\_Material\\_Properties](https://www.researchgate.net/publication/241862538_Thermal_and_Electrical_Properties_of_Nanocomposites_Including_Material_Properties)
8. J. Li, J. Chen, M. Zhu, H. Song, H. Zhang, *Appl. Sci.*, **9**, 2832 (2019). <https://doi.org/10.3390/app9142832>
9. C. Yi, S. Bagchi, F. Gou, C. M. Dmuchowski, C. Park, C. C. Fay, H. B. Chew, Ch. Ke, *Nanotechnology*, **30**, 025706 (2019). <https://doi.org/10.1088/1361-6528/aae874>
10. H. Shen, C. Cai, J. Guo, Z. Qian, N. Zhao, J. Xu, *RSC Adv.*, **6**, 16489 (2016). <https://doi.org/10.1039/c6ra00980h>
11. F. Gou, C. Ke, *Multiscale Science and Engineering*, **1**, 236 (2019). <https://doi.org/10.1007/s42493-019-00021-5>
12. W. Wang, PhD thesis, Department of Materials, Faculty of Science and Engineering, The University of Manchester, UK, 2021.
13. W. Wang, Z. Li, A. J. Marsden, M. A. Bissett, R. J.



- Young, *Composites Science and Technology*, **218**, 109131 (2022).  
<https://doi.org/10.1016/j.compscitech.2021.109131>
14. P. Tatarczak, J. Iwański, A. K. Dąbrowska, M. Tokarczyk, J. Binder, R. Stępniewski, A. Wymolek, *Nanotechnology*, **35**, 175703 (2024).  
<https://doi.org/10.1088/1361-6528/ad18e6>
15. T. Petrova, E. Kirilova, A. Apostolov, R. Vladova, B. Boyadjiev, Analytical modelling of axial strain and interface shear stress distributions in hBN/PMMA nanocomposite under mechanical loading, *Book of abstracts of 7<sup>th</sup> International Scientific Conference "MATHEMATICAL MODELING"*, December 6-9, 2023, Borovets, Bulgaria.  
<https://mathmodel.eu/sbornik/2023.pdf>
16. T. St. Petrova, *Bulg. Chem. Commun.*, **55**(3), 349 (2023). <https://doi.org/10.34049/bcc.55.3.SIMNS05>
17. E. Shopova, N. Vaklieva-Bancheva, BASIC-A genetic algorithm for engineering problems solution, *Computers and Chemical Engineering*, **30**, 1293 (2006).  
<https://doi.org/10.1016/j.compchemeng.2006.03.003>